Supporting Information

Novel approaches for highly selective, room-temperature gas sensors based on atomically dispersed non-precious metals

Renbing Tian[1], Shiyan Wang[2], Xuefeng Hu[3], Jian-Guo Zheng[4], Peng Ji[1], Jun Lin[5], Jing Zhang[6], Mingjie Xu[4], Jun Bao[7], Shouwei Zuo[8], Hui Zhang[9], Wei Zhang[3*], Jinlan Wang[2*] and Liandong Yu[3*]

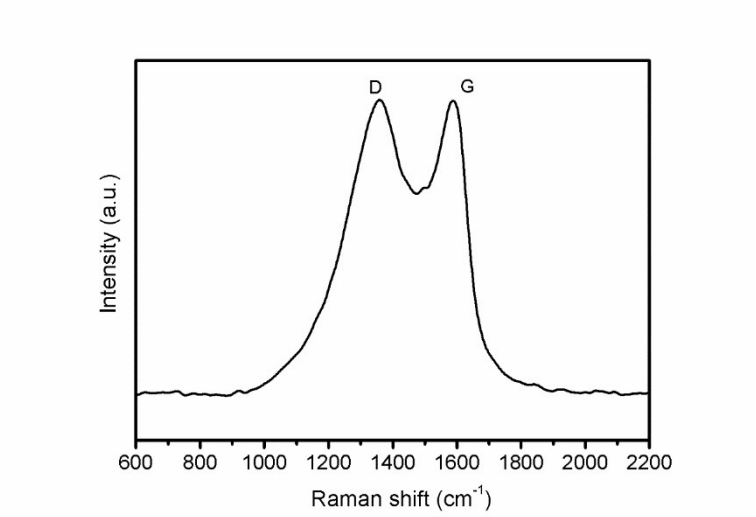

Fig. S1 Raman spectra of AD FeNC.

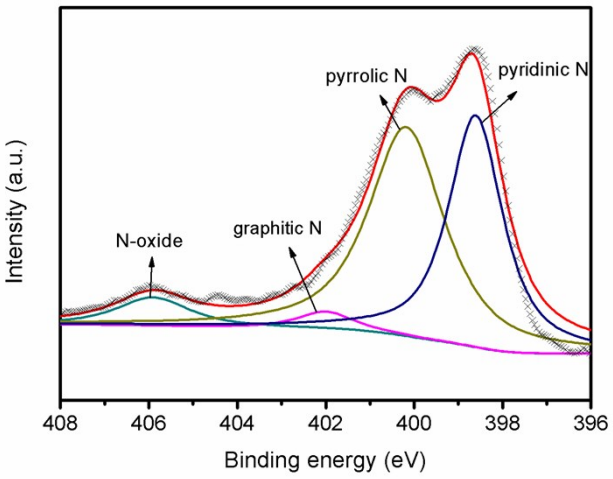

Fig. S2 N 1s XPS spectra of AD FeNC.

In order to further study the morphological stability of the AD FeNC sensor, UV-Vis and SEM characterizations were performed on the AD FeNC material before and after

exposure to 20 ppm NO_2 for 24 hours. As shown in Fig. S3 and S4, no visible changes in SEM morphology images and UV-Vis adsorption profile before and after NO_2 treatment were observed.

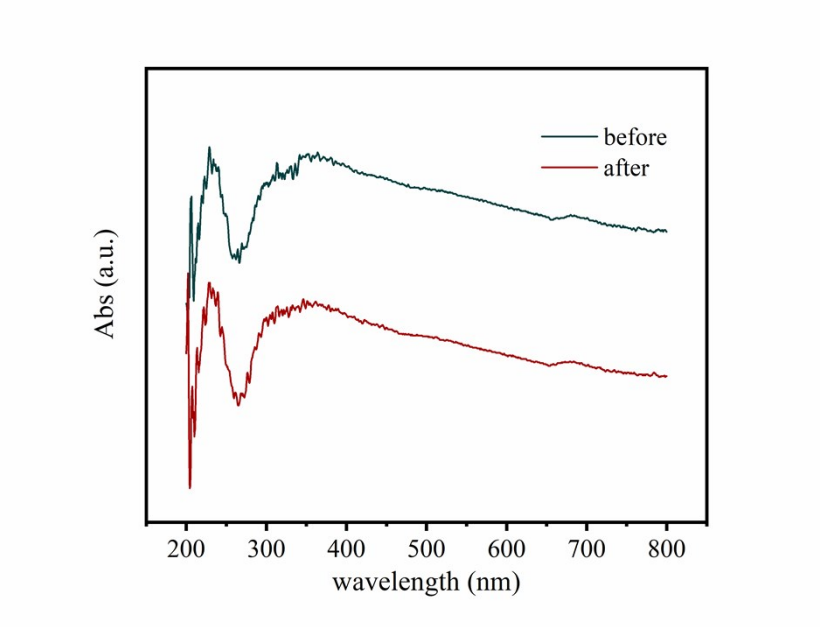

Fig. S3 UV-Vis spectrum of AD FeNC before and after NO_2 treatment

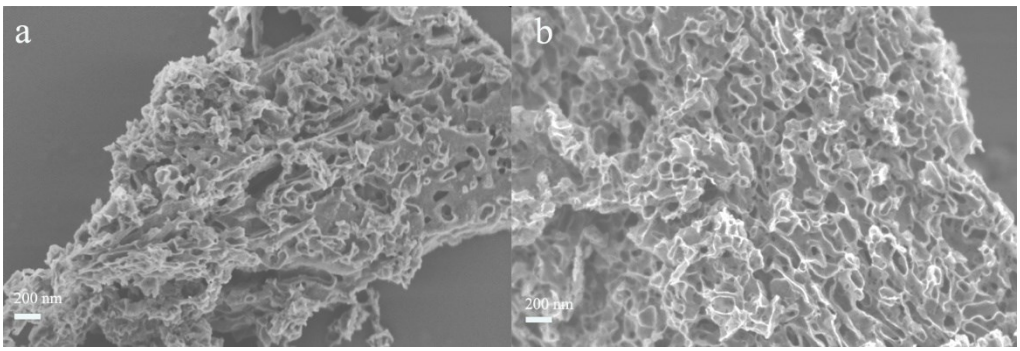

Fig. S4 SEM of AD FeNC before (a) and after (b) NO_2 treatment.

Besides, the influence to gas sensing performance from the thickness of carbon support or the coating film in fabricating gas sensor were also studied. The thickness of carbon support was adjusted by altering the amount of 1,10-phenanthroline Fe(Ⅱ) while the amounts of MgO templates remain unchanged. The more amount of 1,10-phenanthroline Fe(Ⅱ), the thicker of the carbon support. Similarly, the thickness of sensing AD FeNC film was adjusted by varying the drop amount which is the mixture of AD FeNC and ethanol. Different sample was measured under different concentrations of NO_2. The response results of different amount of precursor 1,10-phenanthroline Fe(Ⅱ) were showed in Fig. S5a, while the response of different coating thickness in fabricating gas sensor were displayed in Fig. S5b. It can be found that with the

changes in the thickness of carbon support or the coating film, the sensing response showed no obvious difference. Therefore, the sensing responses are nearly independent to the thickness of both carbon supporter and coating film. In fact, the sensing material to NO_2 in this experiment is only related to the atomic dispersed FeN_4 structure. The changes in the thickness of the films do not alter the distribution of FeN_4, thus film thickness influences on the sensitivity is unexpected

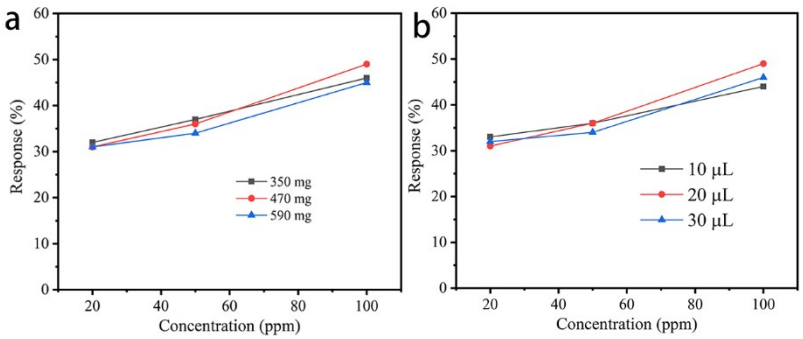

Fig. S5 Response of the AD FeNC sensors fabricated by (a)different amount of precursor 1,10-phenanthroline Fe(Ⅱ) in the case of 20 uL drop and (b)different coating thickness in the case of 470 mg 1,10-phenanthroline Fe(Ⅱ).

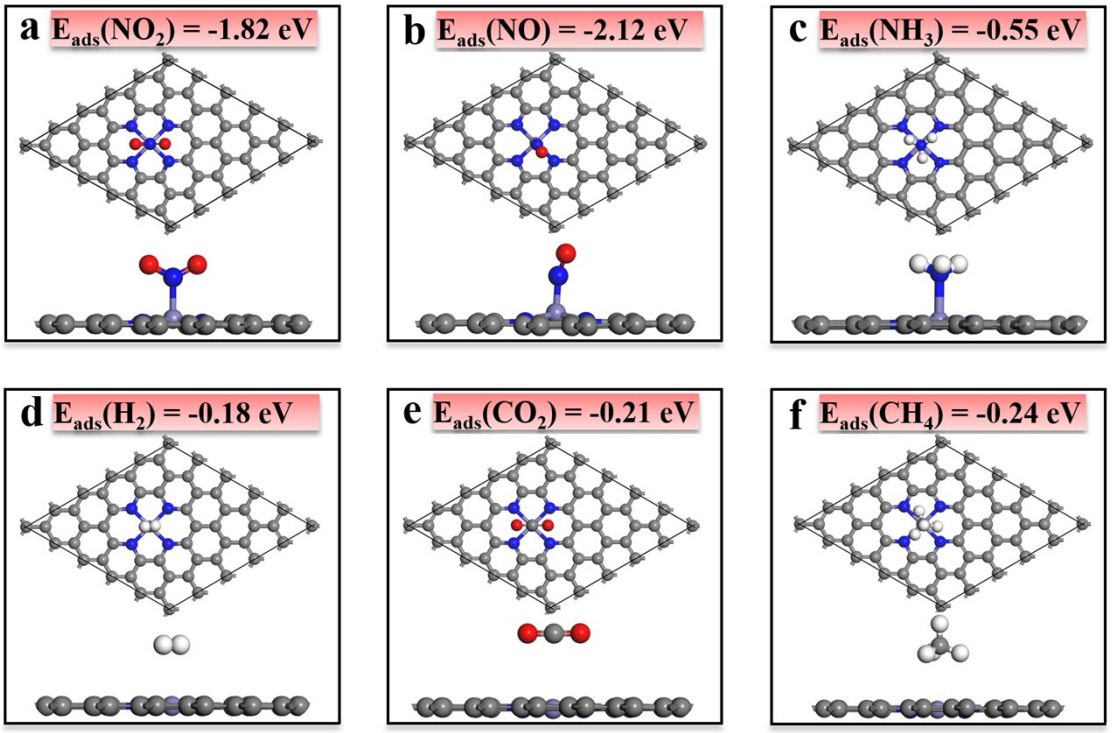

Fig. S6 Adsorption structures and energies of **a** NO_2, **b** NO, **c** NH_3, **d** H_2, **e** CO_2 and **f** CH_4 on AD FeNC. Color scheme: the gray, red, blue, white and purple spheres represent C, O, N, H and Fe atoms, respectively.

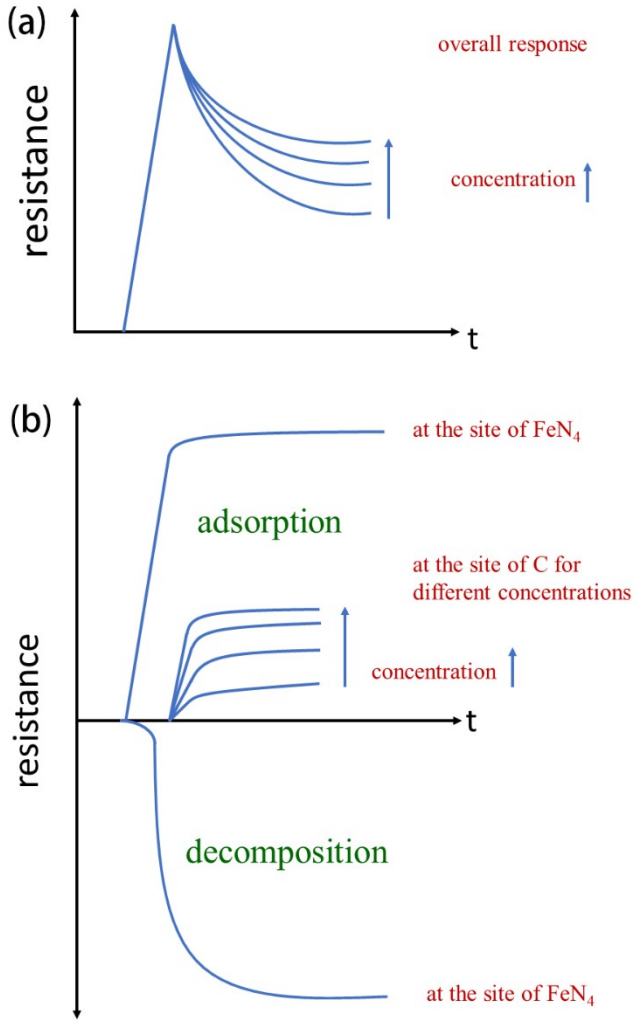

Fig. S7 Diagrammatic sketch of the NO_2 sensing procedures for AD FeNC including decomposition reactions at different gas concentrations.

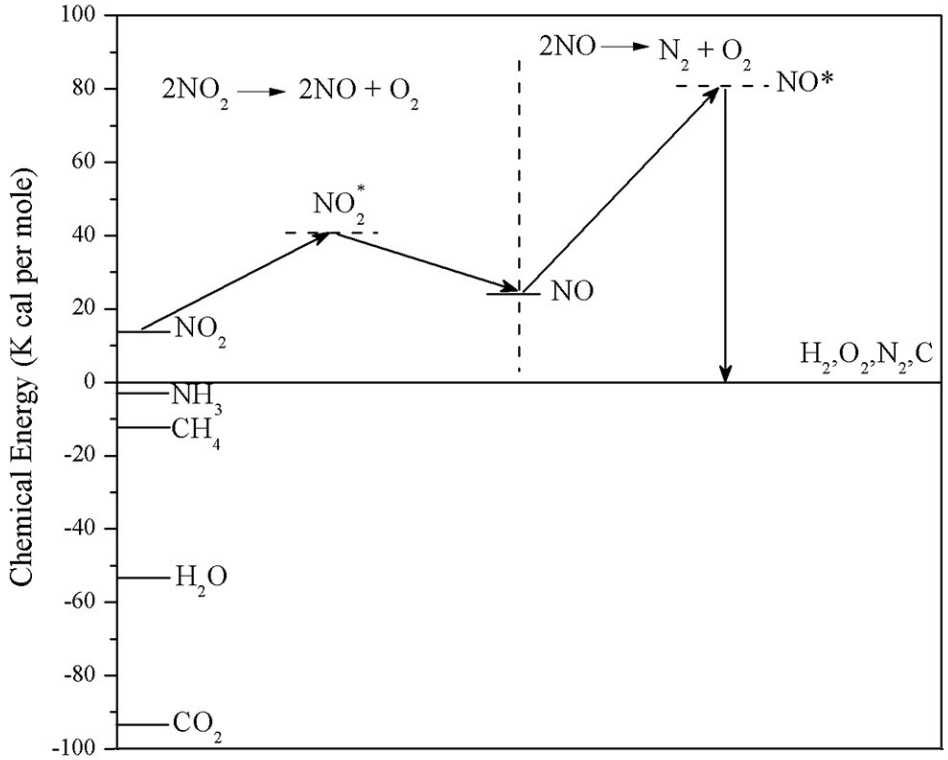

Fig. S8 Free energies of formation of NO and NO_2 are compared with those of other common molecules. Also, the activation energies of NO and NO_2 are shown as a potential barrier to the dissociation reactions given in the diagram. One kilocalorie per mole is equivalent to 0.043 eV per molecule (the activated state and denoted by an asterisk).

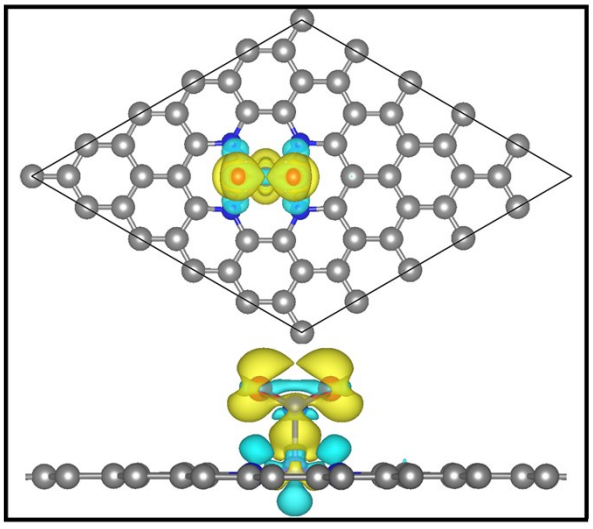

Fig. S9 Top and side views of the charge density difference due to NO_2 adsorption on AD FeNC, where the positive and negative charges are shown in yellow and cyan, respectively. The isosurface value is set to 1×10^{-3} eÅ^{-3}.

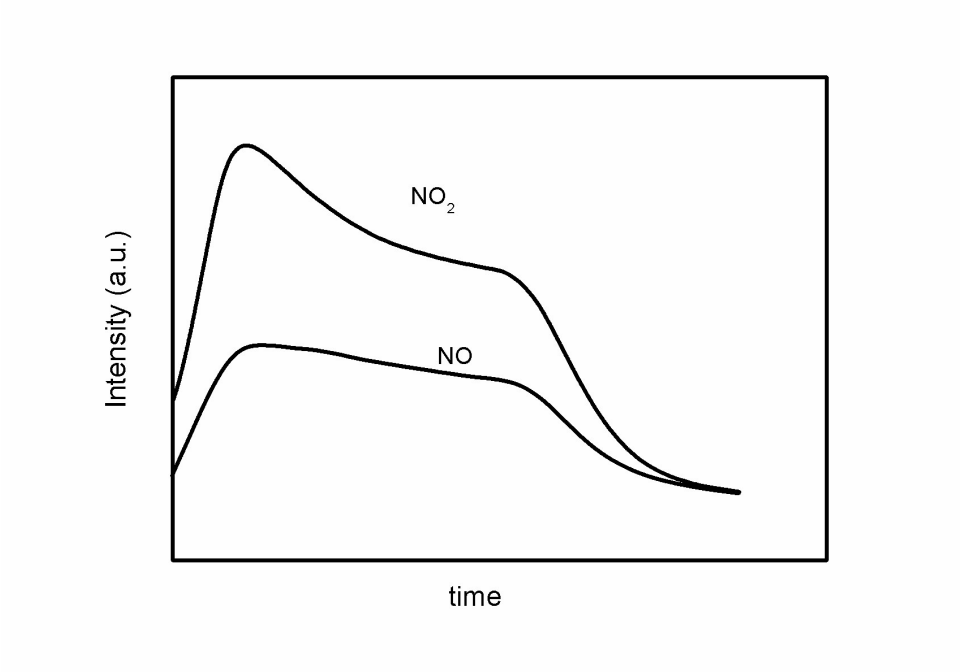

Fig. S10 Sensing performance tendency of the AD FeNC gas sensor to NO_2 and NO with the same concentration of 20 ppm.

Table S1. Charge change of NO_2 and Fe-N-C before and after adsorption

	O in NO_2		N in NO_2	Fe in FeN_4	N in FeN_4			
Before adsorption	+0.38	+0.35	-0.73	-0.99	+1.17	+1.13	+1.17	+1.13
After adsorption	+0.47	+0.48	-0.41	-1.20	+1.16	+1.11	+1.15	+1.10
change	+0.09	+0.13	+0.32	-0.21	-0.01	-0.02	-0.02	-0.03

Table S2. Bond length change of NO_2 and Fe-N-C before and after adsorption

	N-O bond in NO_2		Fe-N bond in FeN_4			
Before adsorption	1.243	1.243	1.900	1.900	1.900	1.900
After adsorption	1.265	1.243	1.912	1.912	1.911	1.911
change	+0.022	-	+0.012	+0.012	+0.011	+0.011

Table S3. Fitting parameters of Fe K-edge EXAFS curves (S_0^2=0.85)

Sample	Path	N	R(Å)	ΔE_0(eV)	$\Delta\sigma^2 \times 10^{-3}$(Å^2)	R-factor(%)
Fe-N-C	Fe-N	4.2	2.00	-4.49±1.72	7.37±1.04	0.19

S_0^2, the amplitude reduction factor; N, coordination number; R, interatomic distance between adsorber and backscatter atoms, ΔE_0, inner potential correction, σ^2, Debye-Waller factor which is used to measure thermal and static disorder in absorber-scatter distances; R, evaluation of the goodness of the fitting.

The fitting parameters are obtained by EXAFS fitting based on the FeN_4 model used in DFT calculation. The k-range was from 2.4 to 7.5 Å while the r-range was from 0.6 to 1.9 Å.